Proceedings of the 1999 IEEE
International Conference on Robotics & Automation
Detroit, Michigan • May 1999

Goldfinger: A Non-Anthropomorphic, Dextrous Robot Hand

Ann M. Ramos, Ian A. Gravagne, and Ian D. Walker
Electrical and Computer Engineering, Clemson University, Clemson, SC 29634

Abstract

In this paper, we describe the hardware and control architecture of a novel four-fingered dextrous robot hand. The benefits of the unusual arrangement of the fingers (which resembles that in raptors and other birds) in the hand are discussed. Kinematic models for the fingers and transmission system are presented. A simulation and real-time control environment has been developed for the hand, and is discussed in the paper. Experiments in dextrous and dynamic manipulation using the hand are also detailed.

1 Background

Over the last few years, there has been much interest in the area of multifingered robot hands and dextrous manipulation. Dextrous multifingered end effectors are potentially ideal for applications requiring a combination of dexterity and versatility for grasping a wide range of objects [4]. The desire to replace existing simple grippers with more dextrous hands has fueled a ongoing surge of activity in the areas of grasping and multifingered end effectors [2],[3].

Since the introduction of the groundbreaking and highly successful Stanford/JPL [7] and Utah/MIT [6] dextrous hand designs in the 1980's, various robot hand designs have been designed, constructed, and tested. Concurrently, a significant body of work in synthesis and analysis of multifingered grasps has been built up. Surveys of these efforts can be found in a number of publications and texts, including [1],[9].

However, at this time, few dextrous hands have been successfully applied to practical applications. Many of the robot hands developed to date have been complex, expensive, and/or bulky, featuring remote actuation via tendons, and have often not been physically robust, with reliability being a problem. There is a strong current interest in developing simpler, more 'minimalist' hand designs [1].

In addition, to date, almost all robot hands have been strongly influenced by the human hand design, and have featured two or more 'fingers' opposing a 'thumb'. While this seems a natural initial design choice, it is not the only one – there are many successful examples in nature of dextrous 'thumbless' manipulation.

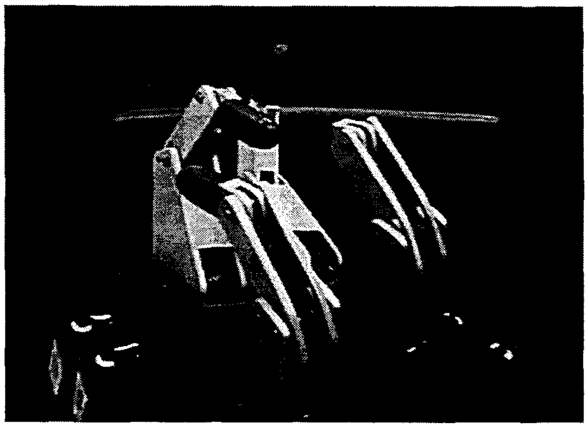

Figure 1: Photo of Goldfinger, a non-anthropomorphic, dextrous robot hand.

From a practical point of view, a special 'thumb' introduces significant complexity to the design and operation of a robot hand, and a simpler design would be appealing. Therefore, from several points of view, it seems natural to investigate the potential of 'thumbless robot hands'.

In this paper, we introduce and describe a new four-fingered dextrous robot hand which incorporates several unique features, resulting in the hand possessing quite novel motions and abilities. Goldfinger, so called for its golden anodized finish on the fingers, has been designed to be fairly dextrous, while at the same time being compact and of simple design. The hand, shown in Figure 1, features a total of twelve degrees of freedom (driven by servomotors via a special linkage system), and was designed and constructed at Rice University in Houston, Texas, while the third author was on the faculty there.

Key design constraints for this project, which was undertaken by Mechanical Engineering seniors at Rice [5], were that the fingers should be modular and simple to construct, and that the cost of the hand should be less than $1000. The linkage system, which is quite unique to the best of our knowledge, enables the actuators to be located compactly within the hand package itself. The final mechanism, including actuators, weighs 2.27 kg. The resulting device, which is quite rugged, has recently been successfully interfaced with a real-time simulation and control environment in the robotics laboratory at Clemson University.

The hand introduced in this paper is unusual in the design and arrangement of its digits in that it does not feature a 'thumb', and in fact its design is more reminiscent of the feet of predatory birds [8]. The (identical) fingers are arranged in two essentially opposing pairs (see Figure 1). This arrangement results in natural motions for the hand which are nonintuitive to humans, and opens up a new realm of previously unconsidered dextrous grasping modes using the hand. Motions of the hand in fact closely resemble that of the talons of raptors. We have previously investigated the grasping behaviors of these birds [8], which prove to be quite dextrous creatures.

In the following sections, we describe the hand and its capabilities in more detail. An analysis of the hand kinematics is followed by details of the actuation scheme. The real-time simulation and control environment developed for the hand is discussed, followed by details of dextrous and dynamic manipulation experiments being conducted using the hand.

2 Hand Architecture

Design simplicity in assembly and machining was a key requirement for the Rice undergraduates who designed and built this hand. As a result, they choose to eliminate the palm from their considerations and instead created a hand which is essentially 2 parallel sets of opposing fingers. This topology does not intuitively lend itself well to human tasks as might an anthropomorphic hand. In fact, the finger configuration conjures up images of other natural manipulators, namely raptorial feet. As was shown in [8], such a four-fingered raptorial hand has a wide range of possible applications. To further explore the mechanics of the hand, let us first consider the individual finger kinematics.

2.1 Finger Kinematics

Taken together, Goldfinger has a total of 12 degrees of freedom, as each of the four fingers has 3 in-

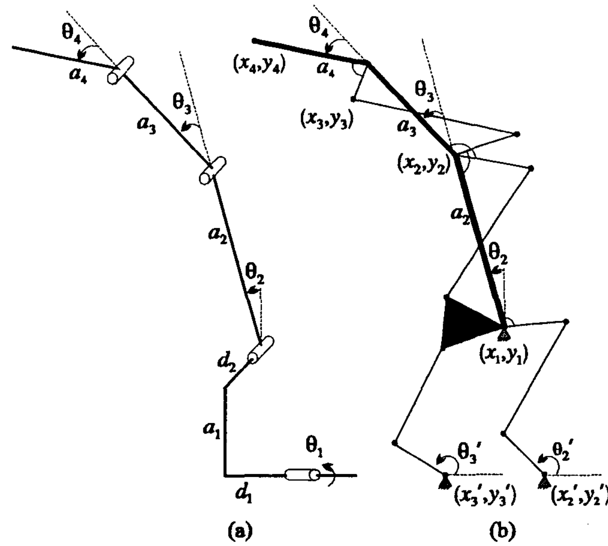

Figure 2: (a) Kinematic model of a single finger. (b) Actuator and D-H model view of the planar robot comprising the 2nd through 4th joints. Dark lines are the D-H parameters, all else is intrinsic to the actuator transmission system.

dependent revolute joints (see Figure 2). The individual fingers are themselves based upon an anthropomorphic model each with four degrees of freedom $\theta_1, \theta_2, \theta_3$, and θ_4, where θ_3 and θ_4 are coupled (see Figure 2(a)). The proximal, or base, joint θ_1 works in abduction/adduction over a range of ± 12 degrees. The remainder of the finger is a constrained redundant planar robot, where there are a total of 3 joints which function in finger flexion/extension. Of these three joints, only the distal joint cannot be separately controlled. The proximal phalange's position depends upon θ_2 (which has functional range of -50 to +57 degrees), and fingertip position relies heavily upon the value of the final independent joint θ_3 (range from -10 to +75 degrees). The third joint in this planar flexion robot, θ_4, is coupled to the previous joint, θ_3, such that the distal phalange follows it, producing a finger which curls in much the same way as does a human finger.

This arrangement allows us to analyze the forward kinematics of each finger in the conventional fashion (i.e. according to the Denavit-Hartenberg convention). For the inverse kinematics, the coupling of joints 3 and 4 complicates the position-level analysis, and has led to our use of iterative (i.e. velocity-level)

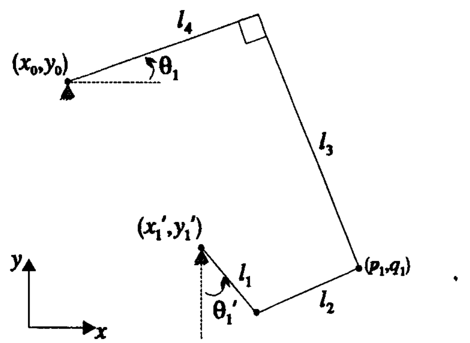

Figure 3: Relationship between joint 1 and its actuator.

solution techniques.

2.2 Finger Actuation

The three independent joints in a finger are directly driven by three RC servos mounted in the base joint. Joints 1 and 2 are each driven by one motor. Joint 3, however, is driven by two motors–the remaining servo and the servo that drives joint 2 as shown in Figure 2(b). This coupling makes the transmission system from the motors to the joints one of the most interesting aspects of this hand from a design perspective.

Let θ_i' be the true actuator angle corresponding to joint position θ_i. Denote counter-clockwise rotation as positive. Each joint linkage system occurs within the same plane as the joint motion. The position of the rotor axis within this plane is fixed and is called $\left(x_i', y_i'\right)$ for the i^{th} motor/joint. In the figures and equations which follow, links in the actuator chain are denoted as l while robot links (in the Denavit-Hartenberg sense) are designated as a. Temporary variables are denoted t, and α represents constant angles. The inverse actuator kinematics, i.e. expressions for θ_i' in terms of θ_i, are presented here as they are necessary for hand control. Additionally, it is more difficult to solve for the forward actuator kinematics in this case. Consequently, we assume that both the position of the origin of each joint i's coordinate frame (x_{i-1}, y_{i-1}) and the joint angle θ_i are known.

In the simplest case, that of joint 1, there are 2 rigid links, l_1 and l_2, to transfer the rotational motion from the rotor to the base joint of the finger, the shell of which is depicted here as l_3 and l_4. For joint 1, the angle θ_1' is measured from vertical (see Figure 3). As stated above, (x_0, y_0) is the origin of the (X_0, Y_0, Z_0) coordinate frame in this plane. If we define the point

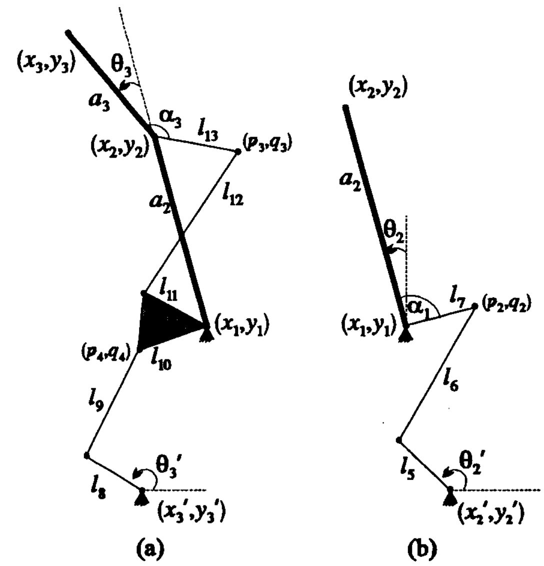

Figure 4: (a) Joint 3's transmission system. (b) Diagram of relation between joint 2 and its actuator.

of connectivity between l_2 and l_3 as (p_1, q_1), then

$$\begin{bmatrix} p_1 \\ q_1 \end{bmatrix} = \begin{bmatrix} x_0 + l_4 \cos\theta_1 + l_3 \sin\theta_1 \\ y_0 + l_4 \sin\theta_1 - l_3 \cos\theta_1 \end{bmatrix}.$$

Let

$$t_1 = \frac{l_2^2 - l_1^2 - (p_1 - x_1')^2 - (q_1 - y_1')^2}{-2l_1\sqrt{(p_1 - x_1')^2 + (q_1 - y_1')^2}}.$$

Then the actuator angle for joint 1 can be found via

$$\theta_1' = \tan^{-1}\left(\frac{p_1 - x_1'}{q_1 - y_1'}\right) - \tan^{-1}\left(\frac{\sqrt{1 - t_1^2}}{t_1}\right). \quad (1)$$

For joints 2 and 3, the actuator angle is measured from the horizontal as shown in Figure 4. For joint 2, as before, two rigid links, l_5 and l_6, transfer rotor motion to the proximal phalange. l_7 represents the bottom edge of the physical link. See Figure 4(b). We assume the positions of the origins of the coordinate frames $(X_1, Y_1, Z_1), (X_2, Y_2, Z_2)$ are known. Projecting these into the plane to obtain $(x_1, y_1), (x_2, y_2)$, we next define the position of the connection between links l_6 and l_7 as

$$\begin{bmatrix} p_2 \\ q_2 \end{bmatrix} = \begin{bmatrix} x_1 - l_7 \sin(\theta_2 - \alpha_1) \\ y_1 + l_7 \cos(\theta_2 - \alpha_1) \end{bmatrix}.$$

The actuator angle for joint 2 is then found from

$$\theta_2' = \tan^{-1}\left(\frac{q_2 - y_2'}{p_2 - x_2'}\right) + \tan^{-1}\left(\frac{\sqrt{1 - t_2^2}}{t_2}\right) \quad (2)$$

where

$$t_2 = \frac{l_6^2 - l_5^2 - (p_2 - x_2')^2 - (q_2 - y_2')^2}{-2l_5\sqrt{(p_2 - x_2')^2 + (q_2 - y_2')^2}}.$$

As the motion is transferred to links further up the system to joint 3, the transmission scheme becomes more complex as shown in Figure 4(a). Once again, actuator rotational motion is transferred via two rigid links l_8 and l_9. Instead of connecting to an application point somewhere on the finger, l_9 attaches to a triangular cam (represented by lengths l_{10} and l_{11} and angle α_2) which pivots about (x_1, y_1). This cam is needed due to routing the linkage system through a jointed finger (i.e. without the cam, joint 3's transmission system would interfere with joint 2's motion). From the top of the cam, we have a second two-link system, where l_{12} is the final link in the actuator chain and l_{13} represents the distance from the application point (p_3, q_3) on the phalange to the (X_2, Y_2, Z_2) origin. Define the temporary angle

$$\varphi_1 = \tan^{-1}\left(\frac{y_3 - y_2}{x_3 - x_2}\right)$$

then this application point is

$$\begin{bmatrix} p_3 \\ q_3 \end{bmatrix} = \begin{bmatrix} x_2 + l_{13}\cos(\varphi_1 - \alpha_3) \\ y_2 + l_{13}\sin(\varphi_1 - \alpha_3) \end{bmatrix}.$$

Next, let

$$t_3 = \frac{l_{12}^2 - l_{11}^2 - (p_3 - x_1)^2 - (q_3 - y_1)^2}{-2l_{11}\sqrt{(p_3 - x_1)^2 + (q_3 - y_1)^2}}$$

so that the angle between l_{11} and the line connecting (p_3, q_3) and (x_1, y_1) is

$$\varphi_2 = \tan^{-1}\left(\frac{\sqrt{1 - t_3^2}}{t_3}\right).$$

The angle between those same points and the horizontal is

$$\varphi_3 = \tan^{-1}\left(\frac{q_3 - y_1}{p_3 - x_1}\right).$$

This gives us the position of the bottom of the triangular cam

$$\begin{bmatrix} p_4 \\ q_4 \end{bmatrix} = \begin{bmatrix} x_1 + l_{10}\cos(\varphi_2 + \varphi_3 + \alpha_2) \\ y_1 + l_{10}\sin(\varphi_2 + \varphi_3 + \alpha_2) \end{bmatrix}.$$

Finally, let

$$t_4 = \frac{l_9^2 - l_8^2 - (p_4 - x_3')^2 - (q_4 - y_3')^2}{-2l_8\sqrt{(p_4 - x_3')^2 + (q_4 - y_3')^2}}$$

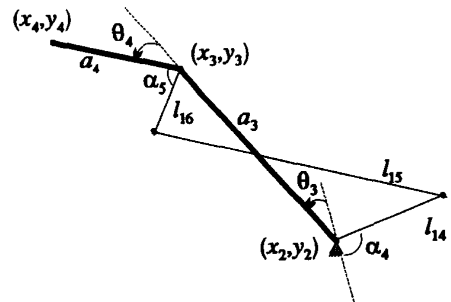

Figure 5: Physical coupling between joints 3 and 4.

so that the actuator angle θ_3' is

$$\theta_3' = \tan^{-1}\left(\frac{q_4 - y_3'}{p_4 - x_3'}\right) + \tan^{-1}\left(\frac{\sqrt{1 - t_4^2}}{t_4}\right). \quad (3)$$

Finally, let us consider the relation between θ_3 and θ_4. The coupling between these joints results in an anthropomorphic curl of the finger during flexion/extension. This 'curl' arises from the linkage system contained within the distal phalange as shown in figure 5. In this figure, l_{14} is the distance from the hinge of the third joint θ_3 to a pivot contained within that phalange, l_{15} is a rigid transmission link, and l_{16} is the distance from a pivot contained within the distal phalange (which acts as a force application point) to the hinge of the fourth joint θ_4. Let the distance from the connection of links l_{14} and l_{15} to the origin of the (X_3, Y_3, Z_3) be

$$t_5 = \sqrt{a_3^2 + l_{14}^2 - 2a_3 l_{14}\cos(180 - \alpha_4 + \theta_3)}.$$

Then temporary angle variable

$$\varphi_4 = \cos^{-1}\left(\frac{t_5^2 - l_{16}^2 - l_{15}^2}{-2l_{15}l_{16}}\right)$$

can be used to define the angle φ_5 between l_{14} and l_{15}, which is

$$\varphi_5 = -\sin^{-1}\left(\frac{l_{16}\sin\varphi_4}{t_5}\right) + \sin^{-1}\left(\frac{a_3\sin(180 - \alpha_4 + \theta_3)}{t_5}\right)$$

Defining the distance from the origin of the (X_2, Y_2, Z_2) coordinate frame to the application point in the distal phalange to be

$$t_6 = \sqrt{l_{14}^2 + l_{15}^2 - 2l_{14}l_{15}\cos\varphi_5},$$

we obtain the angle φ_6 between t_6 and l_{15}, where

$$\varphi_6 = \sin^{-1}\left(\frac{l_{14}\sin\varphi_5}{t_6}\right).$$

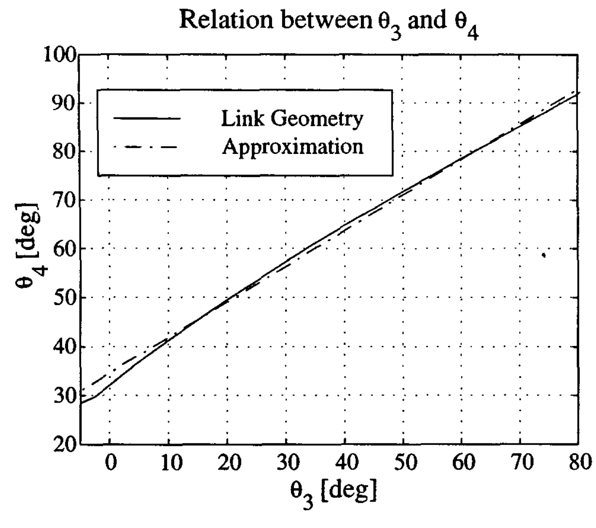

Figure 6: A linear approximation for the relationship between coupled joints 3 and 4 can be found. The approximation is good to within ±1.4 degrees.

Finally, we have

$$\theta_4 = 180 - \alpha_5 - \sin^{-1}\left(\frac{t_6 \sin(\varphi_4 + \varphi_6)}{a_3}\right). \quad (4)$$

Figure 6 depicts this geometric relationship. In practice, we utilize a linear approximation to this function.

Goldfinger contains only a basic sensor set at the present time. The motor gearboxes contain analog angular position sensors; in addition, current sensors give a rough indication of each motor's torque. While still useful, the fact that force applied to the fingertip results in steady-state motor currents requires careful consideration to account for the coupling between some of the joints and motors. Also, torque estimates must be made while the motors are not moving. However, Goldfinger possesses plenty of spare surface area for future sensor additions such as force or proximity sensors. Because there are no active components in the fingertips, these too may be replaced with different shapes and sensor configurations. (An obvious future modification would be to add 'talons' to the fingertips for exploration of the hand's raptorial nature.)

3 System Architecture

Goldfinger's original designers made no provision for real-time control of the hand. Thus, the work at Clemson represents the first time the hand has been automatically controlled. As with any device possessing many degrees of freedom, there is a multitude of data and control signals to track, making it difficult to keep the system simple, maintainable, easy to use and cost effective. We have made several choices which we believe achieve these goals, while still promoting great experimental freedom and flexibility. Figure 7 details the overall picture for real-time control of the hand.

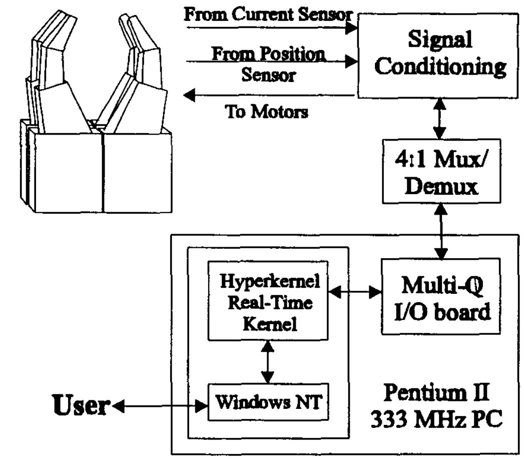

Figure 7: Block diagram of system architecture.

The control and decision algorithms run on a Pentium II, 333MHz PC. The second author's experience with embedded controllers and real-time operating systems motivated the choice to use a 'parallel real-time kernel' which operates in conjunction with Windows NT$^{(R)}$, called HyperKernel^{TM} by Imagination Systems[1]. HyperKernel is not a process running under Windows NT, nor does it encapsulate Windows NT. It is a complete operating system running in a separate, parallel memory space which provides extremely deterministic response to external events, interrupts and timers. As depicted in Figure 7, Windows NT provides the 'front end', where non-critical operations such as the user interface run, communicating with HyperKernel through various mechanisms such as signals, messages and shared memory. This system permits us to achieve the goals of user-friendliness and ease of use because the real-time processes appear to run directly in Windows NT, allowing for a comfortable and familiar environment which is easy to debug, as well as simultaneous operation with other software such as Matlab[2]. Maintainability is also significantly

[1] Imagination Systems, Inc. is a wholly owned subsidiary of Nematron. See www.imagination.com

[2] Matlab is licensed by The Mathworks, Inc. See

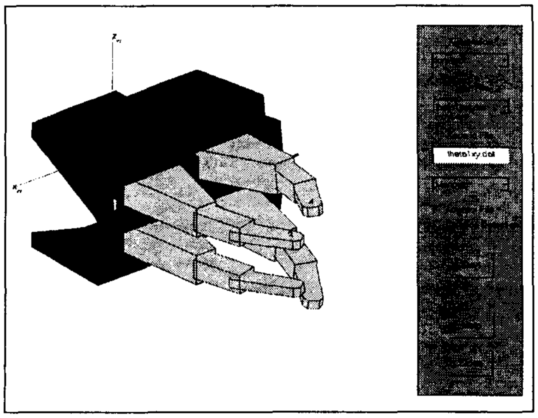

Figure 8: Matlab-based kinematics simulator.

promoted because there is no need to maintain separate platforms for experimental work and general office work. (HyperKernel does not modify the Windows NT hardware abstraction layer.)

Both the user interface and the real-time control and decision code are written in MS Visual C++$^{(R)}$. (It should be noted that HyperKernel does not provide complete support for C++ yet, but the deficiencies are slight enough so as not to hinder good, object-oriented coding.) While the user interface logs incoming data and provides the option to plot variables in pseudo-real-time, HyperKernel addresses external hardware via a MultiQ I/O board by Quanser Consulting[3].

The MultiQ board plugs into a PC ISA slot, and provides an external terminal board with 8 A/D converters, 8 D/A converters, and a host of other digital options including encoder inputs. In the interest of maintaining a cost effective solution, the analog inputs and outputs are externally multiplexed in a 1:4 ratio to provide a total of 32 inputs and outputs, sufficient to control and sense Goldfinger with room to spare.

In this manner, we have synthesized a very cost effective system which is relatively easy to use and maintain and provides significant experimental flexibility. The system has been highly successful in permitting empirical work with Goldfinger, with improvements ongoing.

Figure 9: Goldfinger, mounted on a stand, holding a tennis ball.

4 Preliminary Experiments

A graphics-based hand simulator was written in Matlab. This simulator computes forward and inverse kinematics, corresponding inverse kinematics for the actuator system, and generates a playback movie of the directed trajectories. A simplistic collision detection algorithm was developed to detect potential interference between the fingers. For this purpose, the fingers were modeled as a series of polygons. The normal to each polygon was computed and intersection between component planes are then identified. All experimental work was developed using this simulator.

We initially chose three simple experiments to stress various aspects of Goldfinger and its associated control system. The first tests the accuracy of the kinematics calculations outlined in section 2. The simulator was commanded to provide actuator positions to move the fingers in a manner which essentially 'decoupled' the motions of joints two and three. Recall, joint 3 depends on the position of two motors simultaneously, so the goal was to hold joint 3 constant while varying joint 2. A simple visual inspection of the result confirmed the test.

www.mathworks.com

[3]See www.quanser.com

The second test emphasized the capability of Goldfinger to manipulate objects. The fingers were commanded to manipulate a 9.5cm sphere about six axes, i.e. three rotations and three translations. As the fingers do not yet possess force or torque sensors, the fingertip positions were commanded slightly inside the actual envelope of the sphere in order to maintain contact.

The third test hints at the future direction of experimental work with Goldfinger. We provided a pendulum and set Goldfinger on a stand with the fingers directed upward. The fingers were commanded to strike the pendulum in such a manner as to reverse its direction of motion once every period. This is a simple impact experiment but requires a complex series of quick, precisely timed motions by the fingers. The hand will serve as one of the testbeds for work in dynamic and impact manipulation pursued by the first and third authors. All three tests have been captured on video.

5 Conclusions

We have introduced the hardware and control architecture of a new multifingered robot hand. The hand possesses several novel features which make it a unique platform for dextrous manipulation research. The device has been designed to be a low-cost and medium performance hand. The use of a special actuation linkage structure results in a fairly compact but very rugged mechanical design. The arrangement of the fingers in the hand is strongly non-anthropomorphic. This results in very different 'natural' modes of grasping for the hand, more reminiscent of the behavior of predatory birds, than for traditional robot hands. This, in turn, allows us to approach dextrous grasping tasks in a quite different manner than when using traditional robot hands. In this paper, we have analyzed the kinematics of the hand and summarized the simulation and real-time control environment developed for it. We are currently using the hand as a testbed for impact-based grasping and dynamic manipulation research. Some initial results in this direction have been presented and discussed.

6 Acknowledgments

This work was supported under NSF grant number CMS-9796328, by the U.S. Department of Energy under contract number DE-FG07-97ER14830, and by a grant from the Clemson University Research Grant Committee. Thanks to John Cheatham and the Rice University Mechanical Engineering Department who sponsored the construction of this hand. Additional thanks to Clemson undergraduate Robert Helms for his help in building the multiplexing and PWM boards.

References

[1] Bicchi, A. Hands for Dexterous Manipulation and Powerful Grasping: A Difficult Road Towards Simplicity. In *1996 IEEE International Conference on Robotics and Automation Workshop Notes: Workshop on Minimalism in Robot Manipulation*, Minneapolis, MN, 1996.

[2] Butterfass, J., Hirzinger, G., Knoch S. and H. Liu. DLR's Multisensory Articulated Hand Part I: Hard- and Software Architecture. In *Proceedings of the 1998 International Conference on Robotics and Automation*, Belgium, May 1998, pp 2081-2086.

[3] Caffaz, A. and G. Cannata. The Design and Development of the DIST-Hand Dextrous Gripper. In *Proceedings of the 1998 International Conference on Robotics and Automation*, Belgium, May 1998, pp 2075-2080.

[4] Cutkosky, M.R. and P. McCormick, End Effectors and Tooling, Chapter 14.4 - Robotics, in *CRC Handbook of Mechanical Engineering*, 14.24-14.32.

[5] Crawford, D.S., Blackmon, W.A., Pontefract, J.B. and R.H. Street. *Goldfinger: The Four-Fingered Dextrous Hand.* MECH 408 Final Report, Rice University, April 1992.

[6] Jacobsen, S.C., Iversen, E.K., Knutti, D.F., Johnson, R.T. and K.B. Biggers. Design of the Utah/MIT Dextrous Hand. In *Proceedings of the 1986 International Conference on Robotics and Automation,* San Francisco, 1986, pp 1520-1532.

[7] Mason, M.T. and J.K. Salisbury. *Robot Hands and the Mechanics of Manipulation.* MIT Press, Cambridge, Massachusetts, 1985.

[8] Ramos, A.M. and I.D. Walker. Raptors: Inroads to Multifingered Grasping. To appear in the *Proceedings of the IEEE/RSJ Intelligent Robots and Systems Conference*, Victoria, B.C., 1998.

[9] Walker, I.D. Modeling and Control of Multifingered Hands: A Survey. In *Complex Robotic Systems,* P. Chiacchio and S. Chiaverini, eds., Lecture Notes in Control and Information Sciences Series, Springer-Verlag, London, 1998, pp 129-160.